

# Ring-shaped Andreev billiards in quantizing magnetic fields

J. Cserti,<sup>1,\*</sup> P. Polinák,<sup>1</sup> G. Palla,<sup>2</sup> U. Zülicke,<sup>3,†</sup> and C. J. Lambert<sup>4,‡</sup>

<sup>1</sup>Department of Physics of Complex Systems, Eötvös University, Pázmány Péter sétány 1/A, H-1117 Budapest, Hungary

<sup>2</sup>Biological Physics Research Group of HAS, Eötvös University, Pázmány Péter sétány 1/A, H-1117 Budapest, Hungary

<sup>3</sup>Institute of Fundamental Sciences, Massey University, Private Bag 11 222, Palmerston North, New Zealand

<sup>4</sup>Department of Physics, Lancaster University, Lancaster LA1 4YB, United Kingdom

(Received 11 February 2004; published 21 April 2004)

We present a detailed semiclassical study of a clean disk-shaped insulator–normal-metal–superconductor hybrid system in a magnetic field. It is based on an exact secular equation that we derived within the microscopic Bogoliubov–de Gennes (BdG) formalism. Results obtained from a classification of electron and hole orbits are in excellent agreement with those from an exact numerical diagonalization of the BdG equation. Our analysis opens up different possibilities for determining thermodynamic properties of mesoscopic hybrid systems.

DOI: 10.1103/PhysRevB.69.134514

PACS number(s): 74.45.+c, 03.65.Sq, 05.45.Mt, 73.21.-b

## I. INTRODUCTION

Mesoscopic hybrid systems consisting of normal metals (N) in contact with superconductors (S) exhibit interesting and sometimes counterintuitive equilibrium and transport properties resulting from the interplay between quantum-mechanical phase coherence and superconducting correlations.<sup>1,2</sup> A prominent example is the paramagnetic reentrance effect observed recently in experiments performed by Visani *et al.*<sup>3</sup> on cylindrical S–N proximity samples. While numerous theoretical works<sup>4–7</sup> have addressed this problem, a fully satisfactory explanation of the origin of the sizable paramagnetic contribution to the susceptibility is still lacking. These previous works have studied the spectrum of Andreev bound states formed in planar normal-metal layers in contact with a bulk superconductor, neglecting the effects of cyclotron motion of electrons and holes due to the external magnetic field. Our work presented here extends these studies, taking into account the experimentally relevant circular geometry (shown in Fig. 1) and fully accounting for quantum effects due to the applied magnetic field. Solving exactly the microscopic Bogoliubov–de Gennes equation (BdG),<sup>8</sup> the Andreev levels in a cylindrical NS system are obtained for arbitrary magnetic field. In addition, we give a complete semiclassical description of the spectrum by identifying the possible classical orbits corresponding to the quantum states. This analysis is based on methods developed in our previous work<sup>9</sup> which have been adapted to the case of a finite magnetic field following Ref. 10. Besides being useful for shedding further light on causes for the above-mentioned paramagnetic reentrance effect, our results are intended to serve as a stimulating guide to the investigation of proximity effects in large magnetic fields, which was the focus of several recent experimental<sup>11</sup> and theoretical<sup>12</sup> works.

## II. QUANTUM CALCULATION

We consider a superconducting disk of radius  $R_S$  surrounded by a normal-metal region of radius  $R_N$  shown in Fig. 1. This models the experimentally realized<sup>3</sup> cylindrical

geometry because motion along the axis of the cylinder adds only a trivial kinetic-energy term. The magnetic field is perpendicular to the plane of the disk with a constant value of  $B$  in the N region and zero inside the S region. Thus, the non-zero component of the vector potential in polar coordinates  $(r, \vartheta)$  with symmetric gauge is given by<sup>13</sup>

$$A_\vartheta(r, \vartheta) = B(r^2 - R_S^2)\Theta(r - R_S)/(2r^2), \quad (1)$$

where  $\Theta(x)$  is the Heaviside function.

Excitations in a NS system are described by the BdG equation

$$\begin{pmatrix} H_0 & \Delta \\ \Delta^* & -H_0^* \end{pmatrix} \Psi = E \Psi, \quad (2)$$

where  $\Psi$  is a two-component wave function and  $H_0 = (\mathbf{p} - e\mathbf{A})^2/(2m_{\text{eff}}) + V - E_F$ . Fermi energies and effective masses in the S and N regions are denoted by  $E_F = E_F^{(S)}$ ,  $E_F^{(N)}$ , and  $m_{\text{eff}} = m_S$ ,  $m_N$ , respectively.  $e$  is the electron charge. In the limit  $R_N - R_S \gg \xi_0$ , the superconducting pair potential can be approximated by a step function  $\Delta(\mathbf{r}) = \Delta_0 \Theta(R_S - r)$ , where  $\xi_0 = \hbar v_F / \Delta_0$  is the coherence length and  $v_F$  is the Fermi velocity. Self-consistency of the pair potential is not taken into account, similar to the treatment given in Ref. 14. At  $r = R_N$ , Dirichlet boundary conditions (i.e., an infinite potential barrier) are assumed, while at the NS interface  $r = R_S$ , the presence of a tunnel barrier is mod-

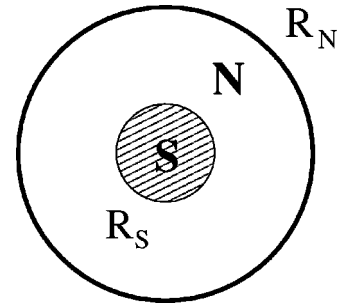


FIG. 1. Schematic view of the system under consideration. A superconducting disk (S) of radius  $R_S$  is surrounded by a normal-metal annulus (N) of outer radius  $R_N$ . A magnetic field is applied perpendicularly to the plane of the disk.

eled by a  $\delta$  potential  $V(r) = U_0 \delta(r - R_S)$ . The energy levels of the system are the positive eigenvalues  $E$  of the BdG equation. In what follows, we consider the energy spectrum below the superconducting gap,  $0 < E < \Delta_0$ . Rotational symmetry of the system implies a separation ansatz for the wave function as a product of radial and angular parts. We choose for the angular part the appropriate angular-momentum eigenfunctions  $e^{im\vartheta}$  with quantum number  $m$ . Then the radial wave functions  $f_m^\pm(r)$  satisfy a one-dimensional BdG equation in the normal region:

$$h_0^{(\pm)}(r) f_m^\pm(r) = \varepsilon f_m^\pm(r), \quad (3a)$$

where

$$h_0^{(\pm)}(r) = -\frac{\hbar \omega_c}{2} \left[ 2 \frac{d}{d\xi} \left( \xi \frac{d}{d\xi} \right) - \frac{m_\pm^2}{2\xi} - \frac{\xi}{2} + m_\pm + \nu_0 \right], \quad (3b)$$

with new dimensionless variables  $\xi = r^2/(2l^2)$  and  $\varepsilon = E/(\hbar \omega_c)$ . The functions  $f_m^\pm(r)$  are, respectively, the electron and hole components of the radial Bogoliubov-de Gennes spinor. Here  $\omega_c = |eB|/m_{\text{eff}}$  is the cyclotron frequency,  $l = \sqrt{\hbar c/|eB|}$  the magnetic length,  $\nu_0 = 2E_F^{(N)}/(\hbar \omega_c)$ ,  $m_\pm = \xi_S \pm m \operatorname{sgn}(eB)$ ,  $\xi_S = R_S^2/(2l^2)$ , and  $\operatorname{sgn}(x)$  denotes the sign function. After transforming the wave functions  $f_m^\pm(r) \rightarrow \xi^{m_\pm/2} e^{-\xi/2} f_m^\pm(r)$ , Eq. (3a) results in a Kummer differential equation,<sup>15</sup> and the ansatz for the wave function in the normal region ( $R_S < r < R_N$ ) can finally be written as

$$\Psi_N(r, \vartheta) = \begin{pmatrix} a_+ \varphi_m^{(N,+)}(r) \\ a_- \varphi_m^{(N,-)}(r) \end{pmatrix} e^{im\vartheta}, \quad (4a)$$

where

$$\begin{aligned} \varphi_m^{(N,\pm)}(r) = & \xi^{m_\pm/2} e^{-\xi/2} \left[ M\left(\frac{1}{2} \mp \varepsilon - \frac{\nu_0}{2}, 1 + m_\pm, \xi\right) \right. \\ & - \left(\frac{\xi_N}{\xi}\right)^{m_\pm} M\left(\frac{1}{2} \mp \varepsilon - \frac{\nu_0}{2} - m_\pm, 1 - m_\pm, \xi\right) \\ & \times \frac{M\left(\frac{1}{2} \mp \varepsilon - \frac{\nu_0}{2}, 1 + m_\pm, \xi_N\right)}{M\left(\frac{1}{2} \mp \varepsilon - \frac{\nu_0}{2} - m_\pm, 1 - m_\pm, \xi_N\right)} \left. \right]. \end{aligned} \quad (4b)$$

Here  $M(a, b, x)$  is Kummer's function<sup>15</sup> and  $\xi_N = R_N^2/(2l^2)$ . These wave functions satisfy the Dirichlet boundary conditions at  $r = R_N$ :

$$\varphi_m^{(N,\pm)}(R_N) = 0. \quad (5)$$

The following symmetries hold:

$$\varphi_m^{(N,-)}(r, \varepsilon, B) = \varphi_m^{(N,+)}(r, -\varepsilon, -B), \quad (6a)$$

$$\varphi_m^{(N,\pm)}(r, \varepsilon, -B) = \varphi_{-m}^{(N,\pm)}(r, \varepsilon, B), \quad (6b)$$

where the dependencies on  $\varepsilon$  and  $B$  are emphasized for clarity.

In the superconducting region  $r < R_S$ , the ansatz for BdG wave functions is given by<sup>9</sup>

$$\Psi_S(r, \vartheta) = \left[ c_+ \begin{pmatrix} \gamma_+ \\ 1 \end{pmatrix} \varphi_m^{(S,+)}(r) + c_- \begin{pmatrix} \gamma_- \\ 1 \end{pmatrix} \varphi_m^{(S,-)}(r) \right] e^{im\vartheta}, \quad (7a)$$

where

$$\varphi_m^{(S,\pm)}(r) = J_m(q_\pm r), \quad (7b)$$

$$q_\pm = k_F^{(S)} \sqrt{1 \pm i\eta}, \quad (7c)$$

$$\eta = \sqrt{\Delta_0^2 - E^2}/E_F^{(S)}, \quad (7d)$$

$$\gamma_\pm = \Delta_0/(E \mp i\sqrt{\Delta_0^2 - E^2}). \quad (7e)$$

Here  $J_m(r)$  is a Bessel function of order  $m$ . The wave functions in the S region satisfy the symmetries:

$$\varphi_m^{(S,-)}(r, \varepsilon) = [\varphi_m^{(S,+)}(r, -\varepsilon)]^*, \quad (8a)$$

$$\gamma_- = \gamma_+^*. \quad (8b)$$

The four coefficients  $a_\pm, c_\pm$  in Eqs. (4) and (7a) are determined from matching conditions at the interface of the NS system.<sup>9</sup> These yield a secular equation for the eigenvalues  $\varepsilon$  of the NS system for fixed mode index  $m$ . Using the fact that the wave functions  $\varphi_m^{(N,+)}$  given in Eq. (4) are real functions and the symmetry relations between the electronic and hole-like component of the BdG eigenspinor, the secular equation can be reduced to

$$\operatorname{Im}\{\gamma_+ D_m^{(+)}(\varepsilon, B) D_m^{(-)}(\varepsilon, B)\} = 0, \quad (9a)$$

where

$$D_m^{(+)}(\varepsilon, B) = \begin{vmatrix} \varphi_m^{(N,+)} & \varphi_m^{(S,+)} \\ [\varphi_m^{(N,+)}]' & Z \varphi_m^{(S,+)} + \frac{m_N}{m_S} [\varphi_m^{(S,+)}]' \end{vmatrix}, \quad (9b)$$






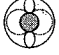
$$D_m^{(-)}(\varepsilon, B) = [D_m^{(+)}(-\varepsilon, -B)]^*. \quad (9c)$$

Here  $Z = (2m_N/\hbar^2) U_0$  is the normalized barrier strength and the prime denotes the derivative with respect to  $r$ . All functions are evaluated at  $r = R_S$ . The energy levels of the NS systems can be found by solving the secular equation (9a) for  $\varepsilon$  at a given quantum number  $m$ . The secular equation derived above is exact in the sense that the usual Andreev approximation is not assumed.<sup>16</sup> An analogous result was found previously<sup>9</sup> for zero magnetic field where the wave functions  $\varphi_m^{(N,\pm)}$  are different.

### III. SEMICLASSICAL APPROXIMATION

We now turn to the semiclassical treatment of the system. For simplicity, we assume a perfect NS interface, i.e.,  $Z = 0$ ,  $E_F^{(S)} = E_F^{(N)}$ , and  $m_S = m_N$ . We follow the method de-

TABLE I. Classification of orbits. The solid/dashed lines correspond to the trajectory of an electron/hole. For the value of turning points  $\tau_{1,2}^{\pm}$ , see Eq. (11).

Type of orbits	$A_+$	$B_+$	$C_+C_-$	$D_+D_-$	$D_+C_-$	$C_+D_-$
						
Conditions	$\tau_S < \tau_1^{\pm}$ $\tau_2^{\pm} < \tau_N$	$\tau_S < \tau_1^{\pm}$ $\tau_N < \tau_2^{\pm}$	$\tau_1^{\pm} < \tau_S$ $\tau_2^{\pm} < \tau_N$	$\tau_1^{\pm} < \tau_S$ $\tau_N < \tau_2^{\pm}$	$\tau_1^{\pm} < \tau_S$ $\tau_2^- < \tau_N$ $\tau_N < \tau_2^+$	$\tau_1^{\pm} < \tau_S$ $\tau_2^+ < \tau_N$ $\tau_N < \tau_2^-$

veloped in Ref. 9, i.e., wave functions which appear in Eq. (9c) are approximated semiclassically. To construct these wave functions in the N region, one can use the standard WKB technique (see, e.g., Refs. 17 and 18) for the radial Schrödinger equation with radial potential given by

$$V_m^{(\pm)}(\tau) = (\tau^2/2 - m_{\pm})^2/\tau^2, \quad (10)$$

where  $\tau = r/l$ . The four turning points (two each for the electron and the hole) can be obtained from  $V_m^{(\pm)}(\tau) = \varepsilon$ . This yields

$$\tau_{1,2}^{\pm} = \sqrt{2(\nu_{\pm} + m_{\pm}) \mp 2[\nu_{\pm}(\nu_{\pm} + 2m_{\pm})]^{1/2}}, \quad (11)$$

where the sign in front of the second term under the square root distinguishes between the first and second turning points for both the electron and the hole, and  $\nu_{\pm} = \nu_0 \pm 2\varepsilon$ . Note that  $\tau_1^{\pm} < \tau_2^{\pm}$ , and the turning points are real if either  $m_{\pm} > 0$  or  $\nu_{\pm} \geq 2m_{\pm}$  for  $m_{\pm} < 0$ . For the electron and hole parts, the cyclotron radius  $\varrho_{\pm}$  and the guiding center  $c_{\pm}$  are given<sup>19</sup> by

$$\varrho_{\pm} = l\sqrt{\nu_{\pm}}, \quad (12a)$$

$$c_{\pm} = l\sqrt{\nu_{\pm} + 2m_{\pm}}. \quad (12b)$$

The relative position of the turning points compared to  $\tau_S = R_S/l$  and  $\tau_N = R_N/l$  enables a classification of possible classical orbits which is summarized in Table I. The different orbits are denoted by capital letters  $A$  to  $D$  and their indices. The  $+/-$  indices correspond to the type of the particles, i.e., electron or hole. The letters distinguish whether the orbit bounces off the inner and/or outer circles or neither of them. In case of type  $A$  the orbits do not bounce off either of the circles which correspond to the Landau states (or cyclotron orbits). The type  $B$  is the so-called skipping orbits (or whispering-gallery modes discussed, e.g., in Ref. 4). In both cases, the orbits do not touch the superconductor and, hence, electron and hole states are not coupled. The other four types of orbits reach the NS interface. In case of type  $C$  the particle touches only the NS interface, while for case of  $D$  the orbits reach both the inner and the outer circles delimiting the N region. In the last four orbits given in Table I, electron and hole alternately Andreev reflect at the NS interface, thus one period of the particle dynamics can be described by two letters with different indices.

In the S region, we approximate the wave function in the same way as in Ref. 9. Substituting the corresponding WKB wave functions and their derivatives into the secular equation (9a) and assuming  $R_S \gg \xi_0$ , we obtain, after tedious but straightforward algebra, the following quantization condition for the semiclassically approximated energy levels:

$$\Phi_m(\varepsilon) = n + \mu. \quad (13)$$

Here  $n$  is an integer and the phase  $\Phi_m(\varepsilon)$  and the Maslov index  $\mu$  are given in Table II. The radial action  $S_m^{(\pm)}$  (in units of  $\hbar/2$ ) of the electron and the hole between  $\tau_1$  and  $\tau_2$  reads

$$S_m^{(\pm)}(\tau_2, \tau_1) = \Theta_m^{(\pm)}(\varepsilon, \tau_2) - \Theta_m^{(\pm)}(\varepsilon, \tau_1), \quad (14a)$$

where

$$\begin{aligned} 2\pi\Theta_m^{(\pm)}(\varepsilon, \tau) = & \sqrt{\tau^2\nu_{\pm} - \left(\frac{\tau^2}{2} - m_{\pm}\right)^2} \\ & - (\nu_{\pm} + m_{\pm}) \arcsin\left(\frac{\nu_{\pm} + m_{\pm} - \tau^2/2}{\sqrt{\nu_{\pm}(\nu_{\pm} + 2m_{\pm})}}\right) \\ & - |m_{\pm}| \arcsin\left(\frac{\tau^2(\nu_{\pm} + m_{\pm}) - 2m_{\pm}^2}{\tau^2\sqrt{\nu_{\pm}(\nu_{\pm} + 2m_{\pm})}}\right). \end{aligned} \quad (14b)$$

TABLE II. Quantization conditions for the different orbits. See also the text.

	$\Phi_m(\varepsilon)$	$\mu$
$A_{\pm}$	$S_m^{(\pm)}(\tau_2^{\pm}, \tau_1^{\pm})$	$\frac{1}{2}$
$B_{\pm}$	$S_m^{(\pm)}(\tau_N, \tau_1^{\pm})$	$\frac{3}{4}$
$C_+C_-$	$S_m^{(+)}(\tau_2^+, \tau_S) - S_m^{(-)}(\tau_2^-, \tau_S) - \frac{1}{\pi} \arccos \frac{E}{\Delta_0}$	0
$D_+D_-$	$S_m^{(+)}(\tau_N, \tau_S) - S_m^{(-)}(\tau_N, \tau_S) - \frac{1}{\pi} \arccos \frac{E}{\Delta_0}$	0
$D_+C_-$	$S_m^{(+)}(\tau_N, \tau_S) - S_m^{(-)}(\tau_2^-, \tau_S) - \frac{1}{\pi} \arccos \frac{E}{\Delta_0}$	$\frac{1}{4}$
$C_+D_-$	$S_m^{(+)}(\tau_2^+, \tau_S) - S_m^{(-)}(\tau_N, \tau_S) - \frac{1}{\pi} \arccos \frac{E}{\Delta_0}$	$-\frac{1}{4}$

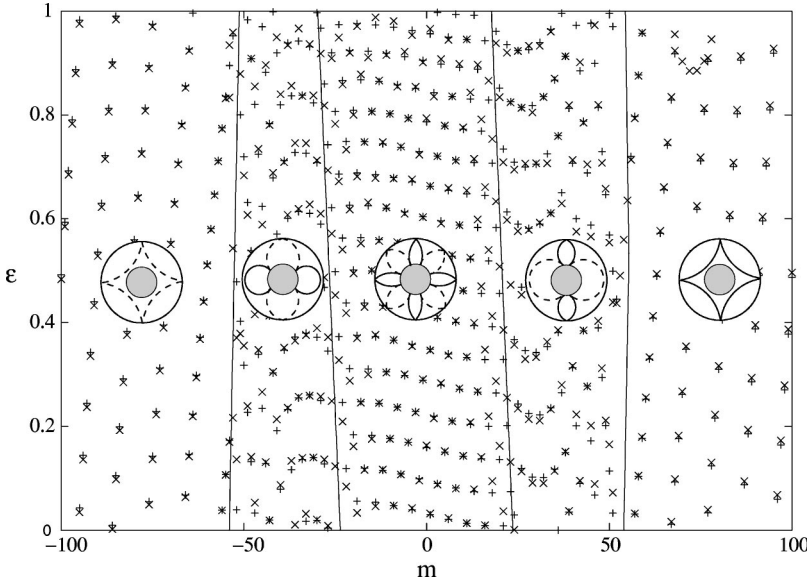


FIG. 2. Exact (crosses) and semiclassical (+ signs) energy levels (in units of  $\Delta_0$ ) obtained from Eqs. (9a) and (13) as functions of quantum number  $m$ . The parameters are  $k_F R_S = 54.0$ ,  $\Phi_{\text{miss}} = 36.5$ ,  $R_S/R_N = 0.45$ , and  $\Delta_0/E_F = 0.1$ . The solid lines represent the border of regions in the  $\varepsilon, m$  plane where the different types of orbits arise. These lines can be obtained from conditions given in Table I. For easy reference, the different types of orbits are depicted in their corresponding regions.

Note that the value of the Maslov index comes out directly from our semiclassical calculation. This result can be interpreted as follows. For orbits of type  $A_{\pm}$ , the quantization condition can be simplified to

$$\nu_{\pm} = 2n + 1 + |m_{\pm}| - m_{\pm}, \quad (15)$$

which coincides with the quantization of the electron/hole cyclotron states of a normal ring in a magnetic field. These are the familiar Landau levels. For orbits of type  $B_{\pm}$ , the radial action between the boundaries of the classical allowed region ( $\tau_1^{\pm}$  and  $\tau_N$ ) is equal to  $n + \mu$ , where  $\mu$  has a contribution  $\frac{1}{4}$  from the soft turning point (at  $\tau = \tau_1^{\pm}$ ) and  $\frac{1}{2}$  from the hard turning point (at  $\tau = \tau_N$ ), resulting in an overall  $\mu = 3/4$ . For cases  $C_+C_-$ ,  $D_+D_-$ ,  $D_+C_-$ , and  $C_+D_-$ , Andreev reflection takes place at the NS interface, resulting in an additional phase shift  $-(1/\pi)\arccos E/\Delta_0$ . The action/Maslov index for the hole is the negative of the action/Maslov index for the electron between the same boundaries.

The conditions for the appropriate boundaries of these types of orbits can be obtained from Table I. The Maslov index is zero for cases  $C_+C_-$  and  $D_+D_-$  because the hole contribution cancels that of the electron. At the outer boundary for type  $D_+C_-$ , there is a hard turning point for the electron and a soft turning point for the hole, resulting in  $\mu = \frac{1}{2} - \frac{1}{4} = \frac{1}{4}$ . Similarly, for  $C_+D_-$ , we have  $\mu = -\frac{1}{2} + \frac{1}{4} = -\frac{1}{4}$ .

#### IV. NUMERICAL RESULTS

In our numerical calculations, it is convenient to use the following parameters for characterizing the experimental situation:  $k_F R_S$  where  $k_F$  is the Fermi wave number,  $\Phi_{\text{miss}} = BR_S^2\pi$  which measures the missing flux due to the Meissner effect,  $R_S/R_N$ , and  $\Delta_0/E_F$ . Figures 2 and 3 show a comparison of the energy levels obtained from the exact quantum calculation with the semiclassical results for two different systems. It is apparent that the semiclassical ap-

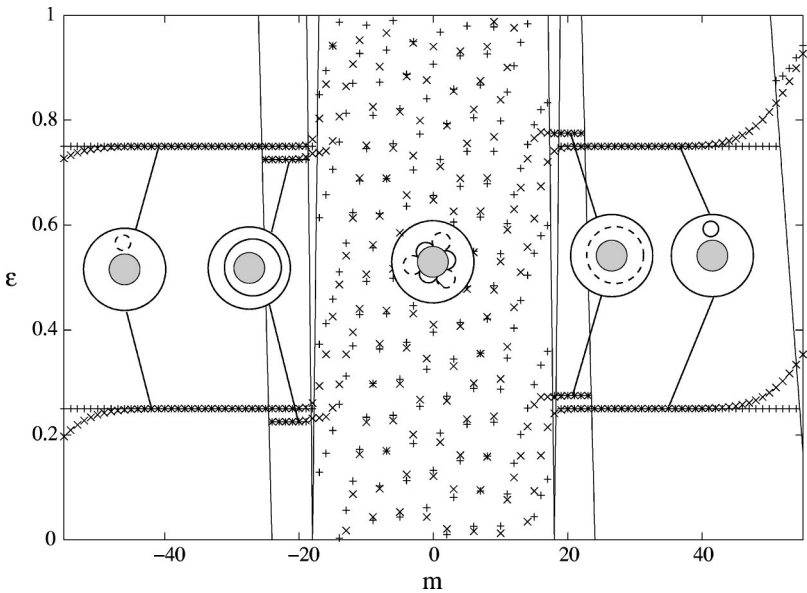


FIG. 3. The same as in Fig. 2 for parameters  $k_F R_S = 18.0$ ,  $\Phi_{\text{miss}} = 4.05$ ,  $R_S/R_N = 0.15$ , and  $\Delta_0/E_F = 0.1$ .



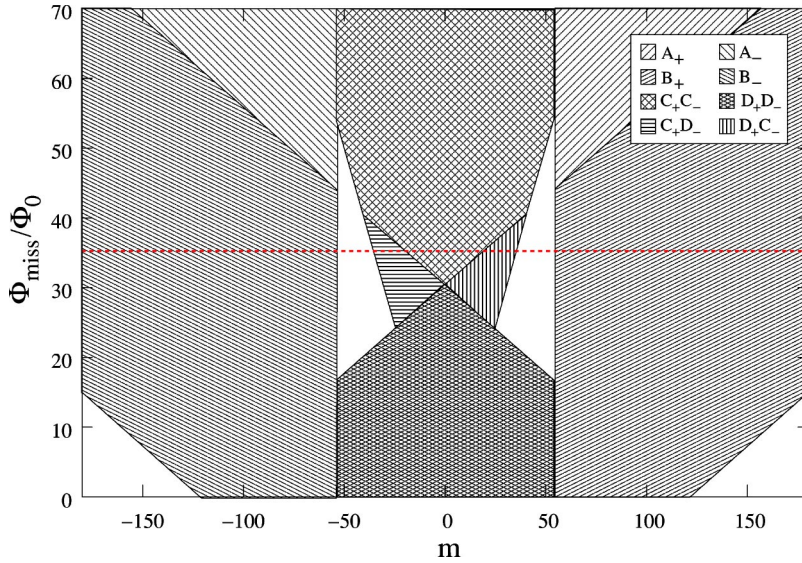


FIG. 4. Regions in parameter space  $\Phi_{\text{miss}}$  (in units of the flux quantum  $\Phi_0 = h/e$ ) and  $m$  where different orbits are realized. The ratio  $R_S/R_N$  and  $k_F R_S$  are the same as in Fig. 2. The horizontal dotted line is at the same missing flux as that in Fig. 2.

proximation is in excellent agreement with the exact quantum result. In Fig. 2, the magnetic field is low such that the cyclotron radius is large compared to  $R_N$ . In this case, no type  $A_{\pm}$  (cyclotron) orbit exists. In contrast, Fig. 3 shows the spectrum when the magnetic field is high enough for the appearance of Landau levels having no dispersion as function of  $m$ . A small difference between quantum and semiclassical results is visible at the border of the region of the  $A_{\pm}$  orbits.

## V. PHASE DIAGRAM

As we discussed in Sec. III, the possibility of existence for the different types of orbits can be determined by considering the relative positions of the turning points compared to  $\tau_S = R_S/l$  and  $\tau_N = R_N/l$ . These conditions are summarized in Table I; they generally depend on geometry and the material (via the parameters  $R_S/R_N$  and  $k_F R_S$ ), the magnetic field (characterized by the missing flux  $\Phi_{\text{miss}}$ ), and the angular-momentum quantum number  $m$ . Given the size and material of the disk, it is possible to decide for each pair of param-

eters  $\Phi_{\text{miss}}, m$  which orbit is realized. It is then possible to draw a phase diagram which is valid for a given disk sample. Examples of such phase diagrams are shown in Figs. 4 and 5 for different geometries distinguished by the same ratios  $R_S/R_N$  as were used in previous Figs. 2 and 3. Note that the weak energy dependence of the turning points translates into the phase diagram being only marginally different for varying  $E < \Delta_0$ . In the figures we have chosen  $E = 0$ . The white regions are classically forbidden, as no classical orbit can be realized at these parameters. The value of the missing flux used in Fig. 2 is indicated as a horizontal line in Fig. 4. This line crosses different regions in the phase diagram. These intersections in  $m$  are the same as those indicated by vertical lines in Fig. 2. Similarly, there is a good agreement between the numerical results and the phase diagram shown in Figs. 3 and 5, respectively.

The phase diagram for the geometry used in the experiment of Ref. 3 is shown in Fig. 6. The experimental situation corresponds to the low-magnetic-field limit where  $\Phi_{\text{miss}} = 0.15h/e$ . There the cyclotron radius is large compared to

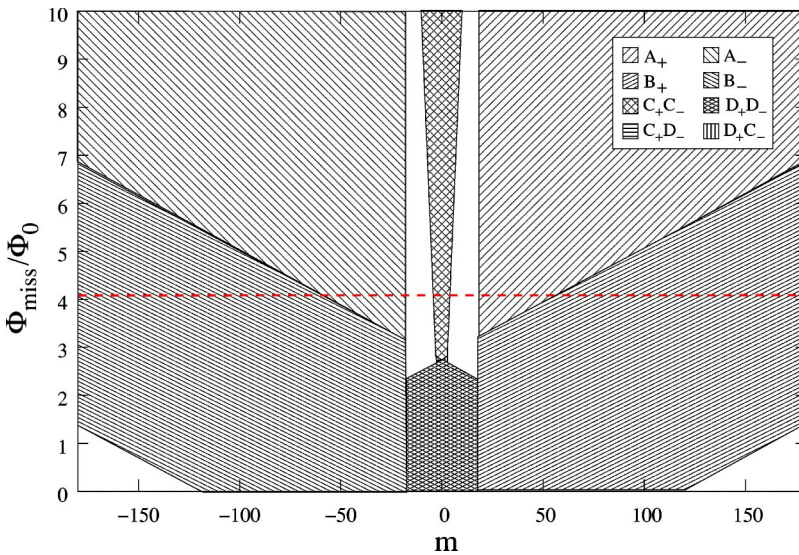


FIG. 5. The same as in Fig. 4 for  $R_S/R_N$  and  $k_F R_S$  corresponding to the results shown in Fig. 3. The horizontal dashed line is at the same missing flux as that in Fig. 3.

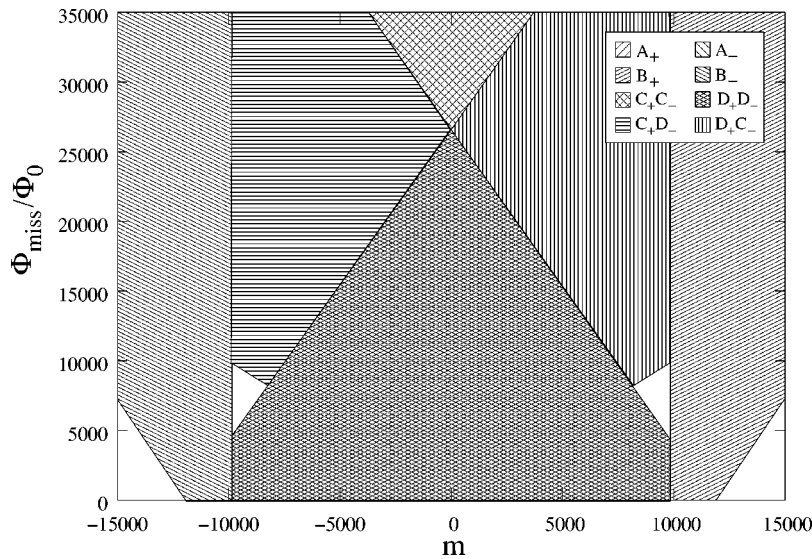


FIG. 6. The phase diagram corresponding to the experiment by Visani *et al.* (Ref. 3). Here  $R_S/R_N=0.7$  and  $k_F R_S=10^4$ .

$R_N$ , and only orbits of type  $B_{\pm}$  and  $D_+D_-$  exist in the semiclassical approximation. Therefore, only these two types contribute to the free energy and, ultimately, to the susceptibility. In a simplified model, these orbits have been included in Bruder and Imry's theoretical study.<sup>4</sup> Thermodynamical quantities such as the magnetic moment or the susceptibility can be determined from the energy levels of the system.<sup>20</sup> However, to fully explain the experimental results,<sup>3</sup> one needs to extend the work presented in this paper. For example, the Meissner effect could be included in a similar way as was done in Ref. 21. The energy levels above the bulk superconducting gap ( $E > \Delta_0$ ) can be obtained by analytical continuation of the secular equation (9a). One can expect a negligible effect from the roughness of the NS interface if the amplitude of the roughness is less than the wavelength of the electrons.<sup>6,22</sup> We expect the spectacular agreement between the fully quantum and the semiclassical treatments to prevail in nonideal situations where deviations from ideal circular geometry occur on a length scale that is smaller than the electron wave length.<sup>23–25</sup>

## VI. CONCLUSIONS

We presented a systematic treatment of an experimentally relevant Andreev billiard in a magnetic field using the

Bogoliubov–de Gennes formalism. An exact secular equation for Andreev bound-state levels was derived which we evaluated both numerically and using semiclassical methods. In particular, a classification of possible classical electron and hole orbits in arbitrary magnetic fields was presented. This provides a useful starting point for subsequent studies of thermodynamic properties because it is possible to obtain the free energy of a NS hybrid system from the quasiparticle energy spectrum. Such an analysis may shed further light on the origin of the recently observed paramagnetic reentrance effect and opens up a whole arena of possibilities to study Andreev billiards in magnetic fields.

## ACKNOWLEDGMENTS

J. Cs. gratefully acknowledges very helpful discussions with C. W. J. Beenakker. This work is supported in part by EU FP6 programme under Contract No. MRTN-CT-2003-504574, the Hungarian-British TeT Grant No. GB-29/01, EPSRC, and the Hungarian Science Foundation OTKA Grant No. TO34832.

\*Electronic address: cserti@galahad.elte.hu

†Electronic address: u.zuelicke@massey.ac.nz

‡Electronic address: c.lambert@lancaster.ac.uk

<sup>1</sup>Physica B **203** (3&4) (1994), special issue on mesoscopic superconductivity, edited by F.W.J. Hekking, G. Schön, and D.V. Averin.

<sup>2</sup>C.J. Lambert and R. Raimondi, J. Phys.: Condens. Matter **10**, 901 (1998).

<sup>3</sup>P. Visani, A.C. Mota, and A. Pollini, Phys. Rev. Lett. **65**, 1514 (1990); A.C. Mota, P. Visani, A. Pollini, and K. Aupke, Physica B **197**, 95 (1994); F.B. Müller-Allinger and A.C. Mota, Phys. Rev. Lett. **84**, 3161 (2000).

<sup>4</sup>C. Bruder and Y. Imry, Phys. Rev. Lett. **80**, 5782 (1998).

<sup>5</sup>A. Fauchère, V. Geshkenbein, and G. Blatter, Phys. Rev. Lett. **82**,

1796 (1999); C. Bruder and Y. Imry, *ibid.* **82**, 1797 (1999); A.L. Fauchère, W. Belzig, and G. Blatter, *ibid.* **82**, 3336 (1999); M. Lisowski and E. Zipper, *ibid.* **86**, 1602 (2001); F. Niederer, A.L. Fauchère, and G. Blatter, Phys. Rev. B **65**, 132515 (2002).

<sup>6</sup>S. Pilgram, W. Belzig, and C. Bruder, Phys. Rev. B **62**, 12462 (2000).

<sup>7</sup>A.V. Galaktionov and A.D. Zaikin, Phys. Rev. B **67**, 184518 (2003).

<sup>8</sup>P.G. de Gennes, *Superconductivity of Metals and Alloys* (Benjamin, New York, 1996).

<sup>9</sup>J. Cserti, A. Bodor, J. Koltai, and G. Vattay, Phys. Rev. B **66**, 064528 (2002).

<sup>10</sup>H. Hoppe, U. Zülicke, and G. Schön, Phys. Rev. Lett. **84**, 1804 (2000).

- <sup>11</sup>H. Takayanagi and T. Akazaki, *Physica B* **249-251**, 462 (1998); T.D. Moore and D.A. Williams, *Phys. Rev. B* **59**, 7308 (1999); D. Uhlisch *et al.*, *ibid.* **61**, 12 463 (2000).
- <sup>12</sup>Y. Takagaki, *Phys. Rev. B* **57**, 4009 (1998); Y. Ishikawa and H. Fukuyama, *J. Phys. Soc. Jpn.* **68**, 954 (1999); Y. Asano, *Phys. Rev. B* **61**, 1732 (2000); N.M. Chtchelkatchev, *JETP Lett.* **73**, 94 (2001).
- <sup>13</sup>L. Solimany and B. Kramer, *Solid State Commun.* **96**, 471 (1995).
- <sup>14</sup>G.E. Blonder, M. Tinkham, and T.M. Klapwijk, *Phys. Rev. B* **25**, 4515 (1982). Regarding self-consistency see, e.g., works cited in Ref. 9.
- <sup>15</sup>A. Abramowitz and I.A. Stegun, *Handbook of Mathematical Functions* (Dover, New York, 1972).
- <sup>16</sup>The Andreev approximation amounts to  $\Delta_0/E_F \ll 1$  and quasiparticles being incident on/reflected from the interface at small enough angles. See, e.g., Ref. 2.
- <sup>17</sup>K. Hornberger and U. Smilansky, *Phys. Rep.* **367**, 249 (2002); K. Hornberger, Ph.D. thesis, Universität München, Germany, 2001.
- <sup>18</sup>S. Klama, *J. Phys.: Condens. Matter* **5**, 5609 (1993).
- <sup>19</sup>C.S. Lent, *Phys. Rev. B* **43**, 4179 (1991).
- <sup>20</sup>C.W.J. Beenakker, in *Transport Phenomena in Mesoscopic Systems*, edited by H. Fukuyama and T. Ando (Springer-Verlag, Berlin, 1992).
- <sup>21</sup>U. Zülicke, H. Hoppe, and G. Schön, *Physica B* **298**, 453 (2001).
- <sup>22</sup>L.A. Falkovsky and S. Klama, *J. Phys.: Condens. Matter* **5**, 4491 (1993).
- <sup>23</sup>M.G. Vavilov and A.I. Larkin, *Phys. Rev. B* **67**, 115335 (2003).
- <sup>24</sup>J.A. Melsen, P.W. Brouwer, K.M. Frahm, and C.W.J. Beenakker, *Europhys. Lett.* **35**, 7 (1996).
- <sup>25</sup>P. Jacquod, H. Schomerus, and C.W.J. Beenakker, *Phys. Rev. Lett.* **90**, 207004 (2003).